

## NUMERICAL ANALYSIS OF ENTROPY GENERATION OF MHD CASSON FLUID FLOW THROUGH AN INCLINED PLATE WITH SORET EFFECT

 **Hiren Deka**,  **Parismita Phukan\***, **Puja Haloi**

*Department of Mathematics, Cotton University, Assam, India*

*\*Corresponding Author e-mail: [parismita12007@gmail.com](mailto:parismita12007@gmail.com)*

Received March 12, 2024; revised April 19, 2024; accepted April, 22, 2024

In this present study, entropy generation for an unsteady MHD Casson fluid flow through an oscillating inclined plate is investigated. Here, along with reaction by chemical and thermal radiation incorporation of Soret effect is also analysed. The solution of the equation which governs the flow problem are obtained by finite difference method (FDM). The features of flow velocity, concentration and temperature are analyzed by designing graphs and their physical behaviour is reviewed in details to study the impact of different parameters on the fluid problem. The skin friction, the rate of heat and mass transfer of the fluid problem also has significant impact under the influence of the parameters. The results indicate that Soret effect and other parameters has considerable impact on an unsteady MHD Casson fluid and on the total entropy due to heat transfer and flow friction.

**Keywords:** *Entropy; Casson; MHD; Soret effect; Thermal radiation*

**PACS:** 44.05.+e, 44.40.+a, 47.11.-j

**MSC2020:** 76W05

### 1. INTRODUCTION

Conservation of energy to produce thermodynamically efficient heat transfer processes has been a topic of interest. The past few years we observed a growing interest in thermodynamics of heat transmission and heat exchange equipments. Heat transmission can be accompanied by entropy generation or thermodynamic irreversibility.

Entropy generation may be due variety of sources such as viscous effects and heat transfer down temperature gradients. It has its huge applications in heat engines, heat pumps, freezers, power plants, and air conditioners. A. Bejan showed how entropy generation rate can be reduced in simple components for heat exchange with an objective to how to reduce useful power. This study will lead the way in which a flow geometry may be selected to reduce generation of entropy. In the intervening years, research work on entropy generation has received considerable attention. Many researchers have contributed their work on entropy generation for a MHD flow. Bejan [1] analyzed the origin of entropy distribution and production for convective heat transmission. Bejan et al. [2] extended entropy generation through heat and fluid flow. Abu-Hijleh [3] numerically analysed the entropy generation for convective flow from a rotating cylinder. The analysis of entropy generation for various physical configurations has been able to draw attentions of researchers and were investigated by many researchers like Baytas[4], Mahmud and Islam [5], Oliveski et al. [6], Hooman et al. [7], Abdelhameed [8], Khan et al. [9], Mansour et al. [10], Sharma et al. [11]. Khan et al. [12] have deliberated the entropy generation of a flow through rotating cone with Dufour and Soret effect's impact. Shit et al. [13] examine the entropy generation for an unsteady flow of nanofluid. Afsana et al. [14] have analysed the entropy generation for a ferrofluid in a wavy enclosure. Qing et al. [15] analysed generation of entropy over a stretching/shrinking porous surface for flow of Casson Nanofluid. Aiboud and Saouli [16] analysed entropy over a stretched surface when a magnetic field is present for MHD viscous flow. Hussain et al. [17] analysed the entropy generation for a double diffusive convection in staggered cavity. Yazdi et al. [18] analysed the entropy generation of parallel open microchannels which is embedded with continuous moving permeable surface. Yazdi et al. [19] extended it for permeable micropatterned surface. Rashidi et al. [20] numerically investigated the generation of entropy over a porous rotating disk with influence of slip factor presented the MHD flow and entropy analysis of heat transmission in a square cavity occupied with Cu–Al<sub>2</sub>O<sub>3</sub>.

The present study of entropy generation for an unsteady MHD Casson fluid flow through an oscillating inclined plate is investigated along with reaction by chemical and thermal radiation and incorporation of Soret effect is also analysed great importance in various fields of energy storage systems and minimization of heat transfer. Heat transfer can be accompanied by entropy generation which has its various applications in different engineering process. Hence, from the literature and its wide applications has motivated the present analysis. The novel aspects of the present analysis are as follows:

- To examine total entropy generations of MHD flow through an inclined plane in addition with the features of flow velocity, temperature and concentration.
- The entropy generation for a free convection is associated with transfer of heat and flow friction of the fluid.
- Along with reaction by chemical and thermal radiation incorporation of Soret effect is also analysed.
- The non-dimensional governing equations are solved numerically by finite difference method in MATLAB.

## 2. STATEMENT

We consider an incompressible one-dimensional unsteady MHD free convection flow with mass and heat transfer of a Casson fluid flowing through an oscillating inclined plate. We consider a viscous fluid with the influence of thermal radiation and reaction by chemical. We consider a coordinate system, where the  $\bar{x}$ -axis represents the vertically upward direction and  $\bar{y}$ -axis is normal to the plate in the direction of the fluid flow. All the existing fluid properties except the influence of density in concentration and temperature are considered to be constant. The induced magnetic field in contrast to the applied magnetic field is considered to be negligible.

Keeping in view the assumptions made above and usual Boussinesq's approximation the equations which governs the flow are:

$$\frac{\partial u^*}{\partial \tau^*} = \nu \left( 1 + \frac{1}{\alpha} \right) \frac{\partial^2 u^*}{\partial \eta^{*2}} + g\beta(T^* - T_{\infty}^*) \cos \gamma + g\beta^*(C^* - C_{\infty}^*) \cos \gamma - \frac{\sigma}{\rho} B_0^2 u^*, \quad (1)$$

$$\frac{\partial T^*}{\partial \tau^*} = \frac{k}{\rho C_p} \frac{\partial^2 T^*}{\partial \eta^{*2}} - \frac{1}{\rho C_p} \frac{\partial q_r^*}{\partial \eta^*}, \quad (2)$$

$$\frac{\partial C^*}{\partial \tau^*} = D_m \frac{\partial^2 C^*}{\partial \eta^{*2}} - kr'(C^* - C_{\infty}^*) + \frac{D_m K_T}{T_m} \left( \frac{\partial^2 T^*}{\partial \eta^{*2}} \right), \quad (3)$$

$$E_g = \frac{k}{T^*{}^2} \left[ \left( \frac{\partial T^*}{\partial \eta^*} \right)^2 \right] + \frac{\mu}{T^*} \left[ \left( \frac{\partial u^*}{\partial \eta^*} \right)^2 \right]. \quad (4)$$

The relevant initial and boundary conditions:

$$u^* = U, T^* = T_w^* + \epsilon e^{i\omega t} (T_w^* - T_{\infty}^*), C^* = C_w^* + \epsilon e^{i\omega t} (C_w^* - C_{\infty}^*) \text{ at } \eta^* = 0, \quad (5)$$

$$u^* \rightarrow 0, T^* \rightarrow 0, C^* \rightarrow 0 \text{ as } \eta^* \rightarrow \infty. \quad (6)$$

where component of velocity in  $x'$  direction is  $u^*$ , the kinematic viscosity is  $\nu$ , the time is  $\tau^*$ , the acceleration caused by gravity is  $g$ , the Casson parameter is  $\alpha$ , the angle of inclination is  $\gamma$ , the thermal expansion coefficient is  $\beta$ , the coefficient of mass is  $\beta^*$ , the fluid temperature is  $T^*$ , the temperature away from plate is  $T_{\infty}^*$ , the temperature near the plate is  $T_w^*$ , the fluid concentration is  $C^*$ , the fluid concentration when it is away from the plate is  $C_{\infty}^*$ , the fluid concentration near the plate is  $C_w^*$ , the magnetic permeability of the fluid is  $\sigma$ , the density of the fluid is  $\rho$ , the coefficient of magnetic field is  $B_0$ , the thermal conductivity is  $k$ , the specific heat at constant pressure is  $C_p$ , the thermal radiation flux is  $q_r^*$ , the chemical reaction rate constant  $kr'$ , the thermal diffusion ratio is  $K_T$ , the coefficient of mass diffusion is  $D_m$ , the mean fluid temperature is  $T_m$ , the scalar constant is  $\epsilon$ , the dimensionless exponential index is  $\omega$ .

The thermal radiation flux gradient  $q_r^*$  under Rosseland approximation is expressed as follows:

$$-\frac{\partial q_r^*}{\partial \eta^*} = 4a\sigma^* (T_{\infty}^* - T_4^*). \quad (7)$$

where  $\sigma^*$  is the Stefan-Boltzmann constant. The difference of temperature within the flow is considered to be into Taylor's series about the free stream temperature. Hence neglecting the higher order terms the result of the approximation is as follows:

$$T_4^* \cong 4T_{\infty}^{*3} T^* - 3T_{\infty}^{*4}$$

We now introduce the following parameters and non-dimensional quantities:

$$\bar{y} = \frac{\eta^* U}{\nu}, \bar{u} = \frac{u^*}{U}, \bar{t} = \frac{\tau^* U^2}{\nu}, \bar{\theta} = \frac{(T^* - T_{\infty}^*)}{T_w^* - T_{\infty}^*}, \bar{\phi} = \frac{(C^* - C_{\infty}^*)}{C_w^* - C_{\infty}^*}, Gr = \frac{g\beta\nu(T_w^* - T_{\infty}^*)}{U^3},$$

$$Gm = \frac{g\beta^*\nu(C_w^* - C_{\infty}^*)}{U^3}, Pr = \frac{\mu C_p}{k}, Sc = \frac{\nu}{D}, M = \frac{\sigma B_0^2 \nu}{\rho U^2}, R = \frac{16a\sigma^* \nu^2 T_{\infty}^{*3}}{U^2 \rho C_p}, S_T = \frac{E_g T_{\infty}^{*2} \nu^2}{k (T_w^* - T_{\infty}^*)^2 U^2},$$

$$\xi = \frac{\mu U^2 T_{\infty}^{*2}}{k (T_w^* - T_{\infty}^*)^2} Kr = \frac{\nu kr'}{U^2}, Sr = \frac{D_m K_T (T_w^* - T_{\infty}^*)}{T_m \nu (C_w^* - C_{\infty}^*)}.$$

Where  $Gm$  is the Grashof number for mass transfer,  $Gr$  is the Grashof number for heat transfer,  $Pr$  is the Prandtl number,  $Sc$  is the Schmidt number,  $Kr$  is the chemical reaction parameter,  $M$  is the Hartmann number and  $R$  is the radiation parameter and  $Sr$  is the Soret number.

Using the non-dimensional quantities, the equations (1) to (4) reduces to:

$$\frac{\partial \bar{u}}{\partial \bar{t}} = \left(1 + \frac{1}{\alpha}\right) \frac{\partial^2 \bar{u}}{\partial \bar{y}^2} + G_1 \bar{\theta} + G_2 \bar{\phi} - M \bar{u}, \tag{8}$$

$$\frac{\partial \bar{\theta}}{\partial \bar{t}} = \frac{1}{Pr} \frac{\partial^2 \bar{\theta}}{\partial \bar{y}^2} - R \bar{\theta}, \tag{9}$$

$$\frac{\partial \bar{\phi}}{\partial \bar{t}} = \frac{1}{Sc} \frac{\partial^2 \bar{\phi}}{\partial \bar{y}^2} - Kr \bar{\phi} + Sr \frac{\partial^2 \bar{\theta}}{\partial \bar{y}^2}, \tag{10}$$

$$S_T = \left(\frac{\partial \bar{\theta}}{\partial \bar{y}}\right)^2 + \xi \left(\frac{\partial \bar{u}}{\partial \bar{y}}\right)^2. \tag{11}$$

Here,  $G_1 = Gr \cos \gamma, G_2 = Gm \cos \gamma$

The non-dimensional form of the corresponding boundary conditions is:

$$\begin{aligned} \bar{u} = 1, \bar{\theta} = 1 + \epsilon e^{i\omega t}, \bar{\phi} = 1 + \epsilon e^{i\omega t} \text{ at } \bar{y} = 0 \\ \bar{u} \rightarrow 0, \bar{\theta} \rightarrow 0, \bar{\phi} \rightarrow 0 \text{ as } \bar{y} \rightarrow \infty \end{aligned}$$

### 3. SOLUTIONS OF THE PROBLEM

In this section, the transformed equations (8) - (11) are coupled non-linear partial differential equations. So, the analytical or exact solutions seem to be not feasible. Finite Difference Method (FDM) is a method which is used to solve differential equations that are quite difficult or impossible to be solved analytically. It is comparatively precise, effective and has better stability characteristics.

The fundamental formula is:

$$\frac{\partial F}{\partial y'} = \lim_{\Delta y' \rightarrow 0} \frac{F(y') - F(y' - \Delta y')}{\Delta y'}$$

The equation above is used to discretise a PDE and then implement a numerical method to solve. The equivalent finite difference scheme for equations (8) to (11) is as follows:

$$\frac{\bar{u}_{i+1,j} - \bar{u}_{i,j}}{\Delta \bar{t}} = \frac{\left(1 + \frac{1}{\alpha}\right) \bar{u}_{i,j+1} - 2\bar{u}_{i,j} + \bar{u}_{i,j-1}}{(\Delta \bar{y})^2} + G_1 \bar{\theta}_{i,j} + G_2 \bar{\phi}_{i,j} - M \bar{u}_{i,j}, \tag{12}$$

$$\frac{\bar{\theta}_{i+1,j} - \bar{\theta}_{i,j}}{\Delta \bar{t}} = \frac{1}{Pr} \left(\frac{\bar{\theta}_{i,j+1} - 2\bar{\theta}_{i,j} + \bar{\theta}_{i,j-1}}{(\Delta \bar{y})^2}\right) - R \bar{\theta}_{i,j}, \tag{13}$$

$$\frac{\bar{\phi}_{i+1,j} - \bar{\phi}_{i,j}}{\Delta \bar{t}} = \frac{1}{Sc} \left(\frac{\bar{\phi}_{i,j+1} - 2\bar{\phi}_{i,j} + \bar{\phi}_{i,j-1}}{(\Delta \bar{y})^2}\right) - Kr \bar{\phi}_{i,j} + Sr \left(\frac{\bar{\theta}_{i,j+1} - 2\bar{\theta}_{i,j} + \bar{\theta}_{i,j-1}}{(\Delta \bar{y})^2}\right), \tag{14}$$

$$S_T = \left(\frac{\bar{\theta}_{i+1,j} - \bar{\theta}_{i,j}}{\Delta \bar{y}}\right)^2 + \xi \left(\frac{\bar{u}_{i+1,j} - \bar{u}_{i,j}}{\Delta \bar{y}}\right)^2. \tag{15}$$

### 4. RESULT AND DISCUSSION

The problem of an unsteady MHD Casson fluid flow past an inclined moving plate in the influence of reaction by chemical, thermal radiation and Soret-effect has been investigated. The mathematical formulation that governs the fluid flow problem is given in equations (1) - (4). Solving this equations, numerical solution has been obtained for the total entropy generation, fluid velocity, concentration, temperature, skin friction, coefficient of the rate of mass and heat transfer in terms of Sherwood number and Nusselt number. Ignoring the imaginary part, numerical results have been displayed in figures and tables. Numerical results obtained using Finite Difference method (FDM) on the governing partial differential equations which analysis the unsteady MHD Casson fluid flow through an oscillating inclined plate with the influence of reaction by chemical, thermal radiation and Soret effect are displayed in graphs and tables. For our computational analysis, we employed  $Gr=5, Gm=5, Pr=.7, R=1, M=5, Sc=.22, Sr=1, Kr=1, T=1.25, \epsilon = .05, \omega = 10$ . unless otherwise stated.

Figure (1)-(4) is portrayed to study the most significant characteristics of the present analysis that is the total entropy generation due to the incorporation of chemical reaction, radiation parameter, Casson parameter and Soret effect. Here, the total entropy for free convection is associated with heat transfer and flow friction. Figure (1) illustrates the chemical reaction influence on total entropy. As the chemical reaction parameter rise the total entropy behaves inversely. Along with it the total entropy decreases with the rise in Hartmann number. Figure (2) illustrates that the increase in the impact of radiation parameter the generation of entropy lowers. Figure (3) shows that the generation of entropy expressed as a function of Hartmann number rise proportionately with the rise in Casson parameter. Figure (4) illustrates that the total entropy lowers with the rise in Soret effect.

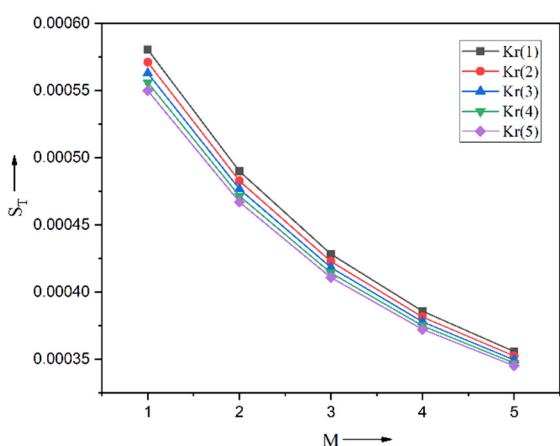


Figure 1. Total entropy with change in chemical reaction

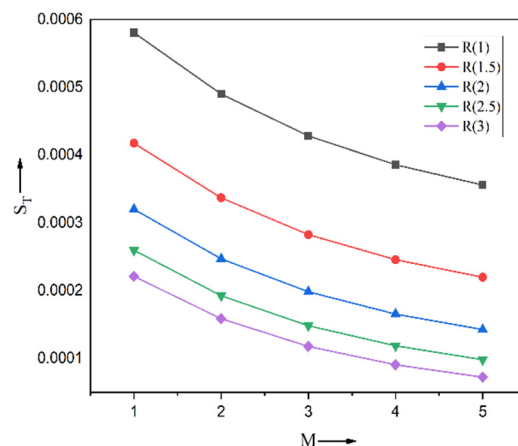


Figure 2. Total entropy with change in radiation parameter

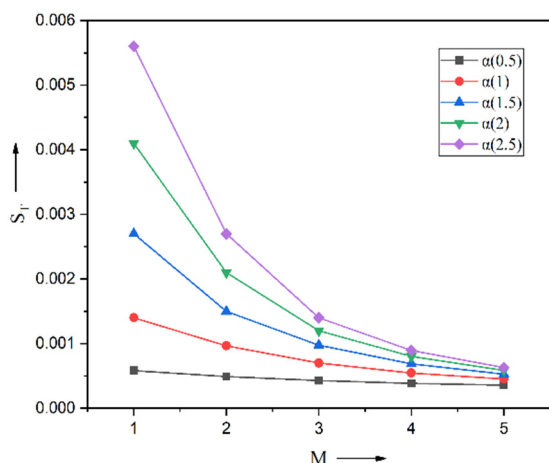


Figure 3. Total entropy with change in Casson parameter

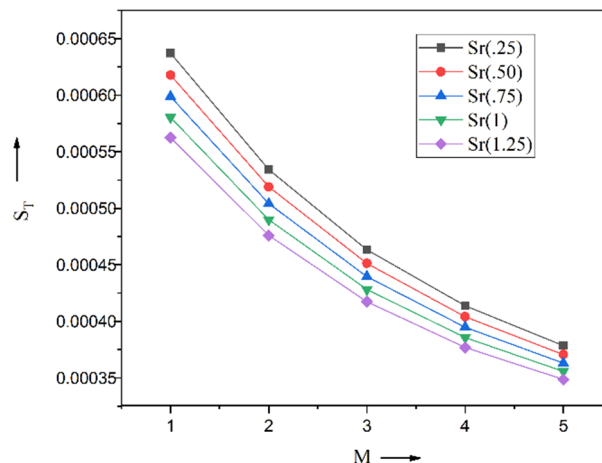


Figure 4. Total entropy with change in Soret effect

Figures (5)-(18) portray the influence of all apposite parameters on the fluid velocity, concentration and temperature. Effect of flow parameters on the skin friction, Nusselt number and Sherwood number are also illustrated in tabular form. Figures (5) and (6) demonstrates the variation of temperature against  $y$  with the impact of radiation parameter ( $R$ ) and Prandtl number ( $Pr$ ) on temperature profile.

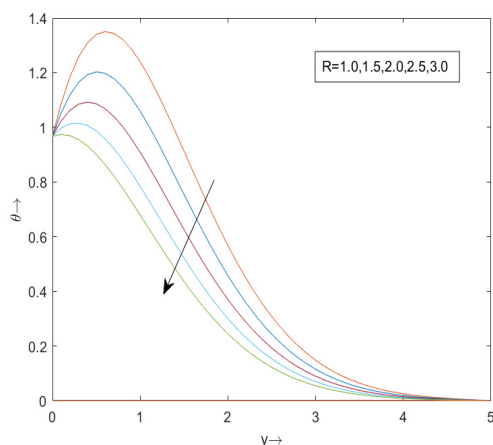


Figure 5. Variation of radiation parameter on temperature

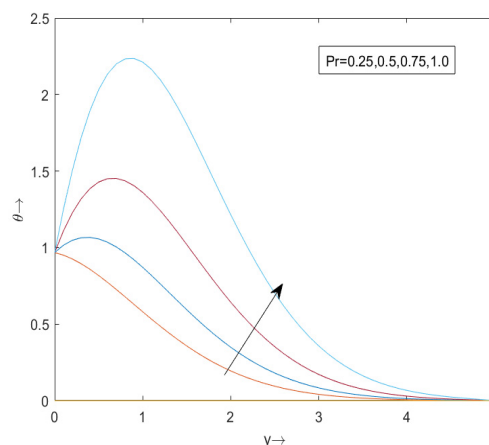


Figure 6. Variation of Prandtl number on temperature

The degree of temperature of fluid falls with the rise in radiation parameter and rises with the rise in Prandtl number. Figures (7)-(13) exhibit the effect of different parameters on velocity profile. It is seen from the Figure (7) that velocity profile decreases with the rise in Chemical reaction parameter  $Kr$  and from the Figure (8) one can find that the velocity increases proportionately with the Prandtl number. Hartmann number  $M$  is the ratio of electromagnetic forces to inertia forces. The Schmidt number  $Sc$  differentiates the relative thickness of velocity and the concentration boundary layers.

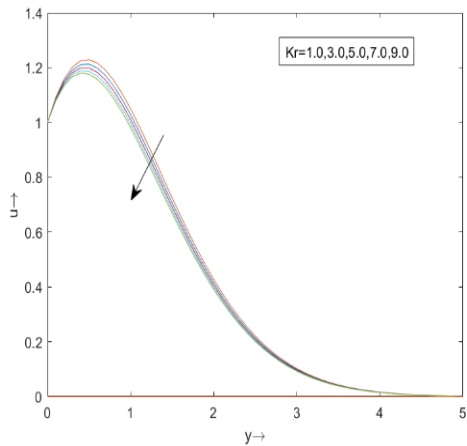


Figure 7. Variation of Chemical reaction parameter on velocity

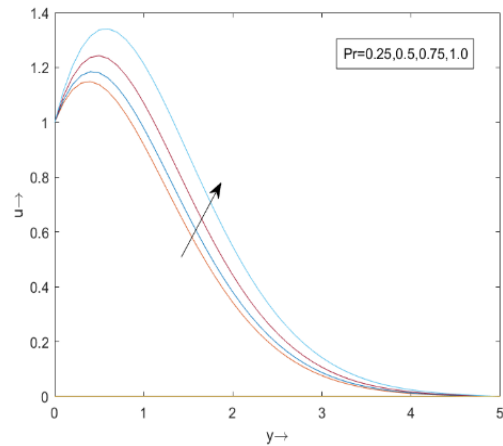


Figure 8. Variation of Prandtl number on velocity

Figure (9) and (10) portray that velocity profile decelerated with the increase in Hartmann number and Schmidt number.

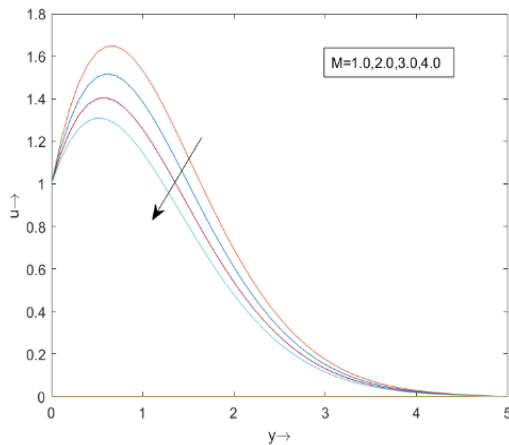


Figure 9. - Variation of Hartmann number on velocity

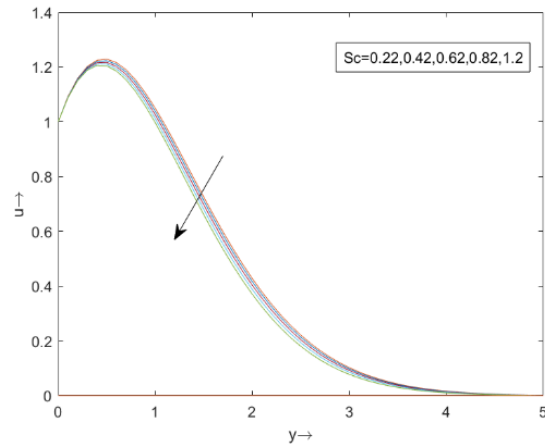


Figure 10. Variation of Schmidt number on velocity

From Figure (11) it is observed that, the velocity profile rise with the rise in casson parameter. The thermo-diffusion or Soret effect  $Sr$  may take place due to the presence of temperature gradient. It is evident from the Figure-(12) that, velocity falls with the rise in Soret number and the Figure (13) shows that as the radiation parameter increases, the velocity profile decreases. Figures (14)-(18) demonstrate the change in concentration profile with the influence of different parameters. It is observed that in the figure-(14) the concentration decreases as the Schmidt number increases. Figure (15) and (16) shows that concentration decreases with the increase in the chemical reaction parameter and the Soret effect. Figure (17) shows that concentration profile increases proportionately with radiation parameter. Figure (18) depicts that concentration profile decreases with the increase in Prandtl number.

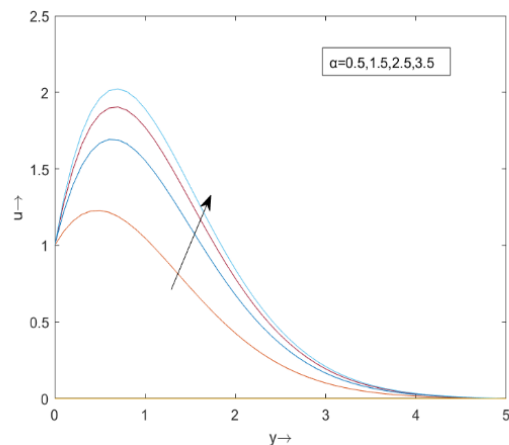


Figure 11. -Variation of Casson parameter on velocity

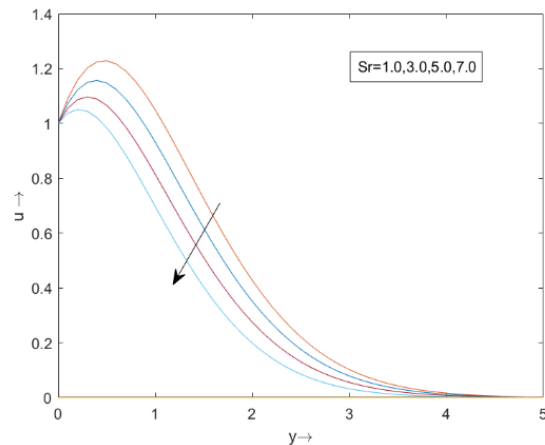


Figure 12. Variation of Soret number on velocity

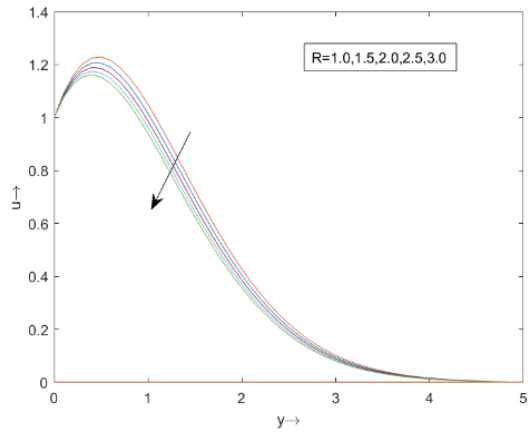


Figure 13. Variation of Radiation parameter on velocity

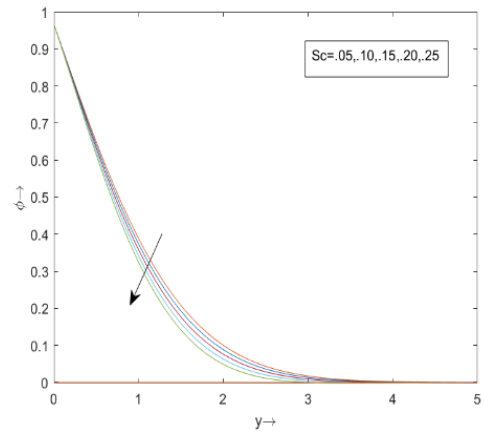


Figure 14. Variation of Schmidt number on concentration

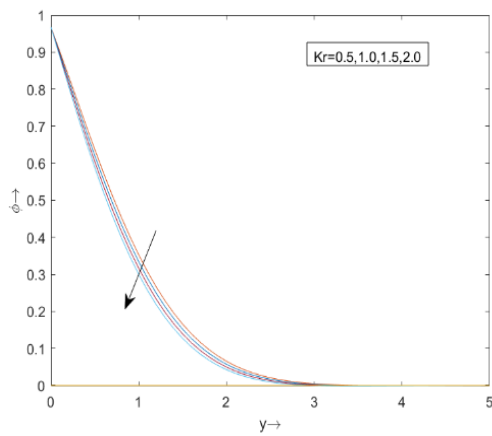


Figure 15. Variation of Chemical reaction parameter on concentration

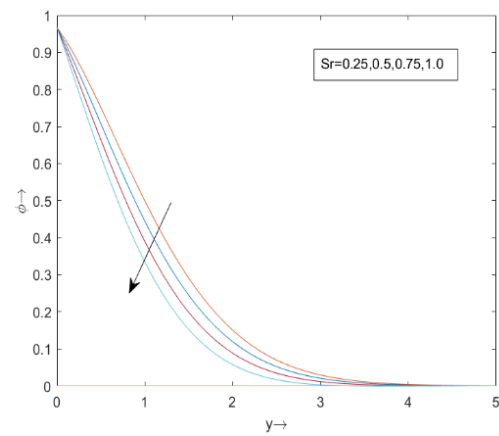


Figure 16. Variation of Soret effect on concentration

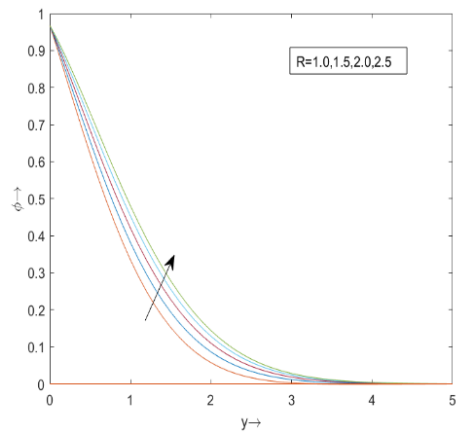


Figure 17. Variation of radiation parameter on concentration

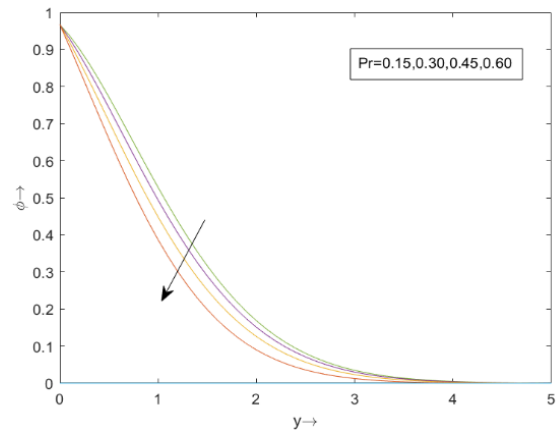


Figure 18. Variation of Prandtl number on concentration

Table 1. Nusselt Number

Pr	R	Nusselt Number
0.25	1.0	-0.1733
0.50	1.0	0.4975
0.75	1.0	1.4629
1.00	1.0	2.9249
0.70	1.0	1.2382
0.70	1.5	0.8860
0.70	2.0	0.5783
0.70	2.5	0.3077
0.70	3.0	0.0684

**Table 2.** Sherhood Number

Pr	R	Sc	kr	Sr	Sherhood Number
<b>0.25</b>	1.0	0.22	1.0	1.0	-0.3623
<b>0.50</b>	1.0	0.22	1.0	1.0	-0.5297
<b>0.75</b>	1.0	0.22	1.0	1.0	-0.7701
<b>1.00</b>	1.0	0.22	1.0	1.0	-1.1326
0.70	<b>1.0</b>	0.22	1.0	1.0	-0.7143
0.70	<b>1.5</b>	0.22	1.0	1.0	-0.6266
0.70	<b>2.0</b>	0.22	1.0	1.0	-0.5499
0.70	<b>2.5</b>	0.22	1.0	1.0	-0.4824
0.70	1.0	<b>0.22</b>	1.0	1.0	-0.7143
0.70	1.0	<b>0.42</b>	1.0	1.0	-0.7722
0.70	1.0	<b>0.62</b>	1.0	1.0	-0.8428
0.70	1.0	<b>0.82</b>	1.0	1.0	-0.9263
0.70	1.0	0.22	<b>1.0</b>	1.0	-0.7143
0.70	1.0	0.22	<b>3.0</b>	1.0	-0.9096
0.70	1.0	0.22	<b>5.0</b>	1.0	-1.0819
0.70	1.0	0.22	<b>7.0</b>	1.0	-1.2354
0.70	1.0	0.22	1.0	<b>2.0</b>	-1.1885
0.70	1.0	0.22	1.0	<b>4.0</b>	-2.1371
0.70	1.0	0.22	1.0	<b>6.0</b>	-3.0856
0.70	1.0	0.22	1.0	<b>8.0</b>	-4.9827

**Table 3.** Skin friction

Pr	R	Sc	kr	Sr	M	$\alpha$	Skin friction
<b>0.25</b>	1.0	0.22	1.0	1.0	5.0	0.5	0.6972
<b>0.50</b>	1.0	0.22	1.0	1.0	5.0	0.5	0.7922
<b>0.75</b>	1.0	0.22	1.0	1.0	5.0	0.5	0.9268
<b>1.00</b>	1.0	0.22	1.0	1.0	5.0	0.5	1.1235
0.70	<b>1.0</b>	0.22	1.0	1.0	5.0	0.5	0.8958
0.70	<b>1.5</b>	0.22	1.0	1.0	5.0	0.5	0.8468
0.70	<b>2.0</b>	0.22	1.0	1.0	5.0	0.5	0.8036
0.70	<b>2.5</b>	0.22	1.0	1.0	5.0	0.5	0.7654
0.70	1.0	<b>0.22</b>	1.0	1.0	5.0	0.5	0.8958
0.70	1.0	<b>0.42</b>	1.0	1.0	5.0	0.5	0.8866
0.70	1.0	<b>0.62</b>	1.0	1.0	5.0	0.5	0.8769
0.70	1.0	<b>0.82</b>	1.0	1.0	5.0	0.5	0.8670
0.70	1.0	0.22	<b>1.0</b>	1.0	5.0	0.5	0.8958
0.70	1.0	0.22	<b>3.0</b>	1.0	5.0	0.5	0.8589
0.70	1.0	0.22	<b>5.0</b>	1.0	5.0	0.5	0.8265
0.70	1.0	0.22	<b>7.0</b>	1.0	5.0	0.5	0.7981
0.70	1.0	0.22	1.0	<b>2.0</b>	5.0	0.5	0.8069
0.70	1.0	0.22	1.0	<b>4.0</b>	5.0	0.5	0.6292
0.70	1.0	0.22	1.0	<b>6.0</b>	5.0	0.5	0.4514
0.70	1.0	0.22	1.0	<b>8.0</b>	5.0	0.5	0.2737
0.70	1.0	0.22	1.0	1.0	<b>1.0</b>	0.5	1.9257
0.70	1.0	0.22	1.0	1.0	<b>2.0</b>	0.5	1.6283
0.70	1.0	0.22	1.0	1.0	<b>3.0</b>	0.5	1.3601
0.70	1.0	0.22	1.0	1.0	<b>4.0</b>	0.5	1.1171
0.70	1.0	0.22	1.0	1.0	5.0	<b>0.5</b>	0.8958
0.70	1.0	0.22	1.0	1.0	5.0	<b>1.5</b>	2.1472
0.70	1.0	0.22	1.0	1.0	5.0	<b>2.5</b>	2.6835
0.70	1.0	0.22	1.0	1.0	5.0	<b>3.5</b>	2.9814

### 5. CONCLUSIONS

Following are the conclusion of the present investigation:

- The total entropy lowers with the rise in chemical reaction parameter, radiation parameter and Soret effect.
- Entropy generation rise proportionately with the rise in Casson parameter.
- The degree of temperature falls with the increasing radiation parameter and rise with the increasing Prandtl number.
- The velocity of fluid flow is decelerated with increasing reaction by chemical, Hartmann number, Schmidt number, Soret effect and radiation parameter and is accelerated proportionately with the Prandtl number and Casson parameter

- The level of concentration of the fluid rises with the rise in radiation parameter and falls with the rise in Schmidt number, reaction by chemical, Soret effect and Prandtl number.
- Skin friction coefficient increases proportionately with Prandtl number and casson parameter.
- Skin friction is decreasing with the increasing Hartmann number, radiation parameter, Schmidt number, reaction by chemical and Soret effect.
- The rate of heat transfer rise with the increasing Prandtl number, whereas it is reduced with the increasing radiation parameter.
- The rate of mass transfer rise with the increasing radiation parameter, whereas it falls with the increasing Prandtl number, Soret effect, Schmidt number and reaction by chemical.

#### Nomenclature

$\nu$ = kinematic viscosity	$K_T$ = thermal diffusion ratio
$\alpha$ = casson parameter	$T_m$ = mean fluid temperature
$\gamma$ = angle of inclination	$q'_r$ = radiative heat flux
$\xi$ = ratio of viscous to thermal entropy	$u$ = dimensionless velocity
$\beta$ = thermal expansion coefficient	$\theta$ = nondimensional temperature
$\beta^*$ = mass expansion coefficient	$\phi$ = nondimensional concentration
$g$ = acceleration due to gravity	$Gr$ = Grashof number for heat transfer
$C'$ = species concentration	$Gm$ = Grashof number for mass transfer
$C'_\infty$ = fluid concentration far away from the wall	$Pr$ = Prandtl number
$T'$ = temperature of the fluid	$Sc$ = Schmidt number
$T'_\infty$ = fluid temperature far away from the wall	$M$ = Hartmann number
$\sigma$ = electrical conductivity	$R$ = radiation parameter
$\rho$ = fluid density	$Kr$ = chemical reaction parameter
$B_0$ = magnetic field	$Sr$ = Soret number
$C_p$ = specific heat at constant pressure	$\tau$ = skin friction
$D_m$ = mass diffusivity	$Nu$ = Nusselt number
$Kr'$ = chemical reaction rate constant	$Sh$ = Sherwood number

#### ORCID

©Hiren Deka, <https://orcid.org/0009-0002-1512-5984>; ©Parimita Phukan, <https://orcid.org/0000-0002-2116-5571>

#### REFERENCES

- [1] A. Bejan, "A study of entropy generation in fundamental convective heat transfer," *Journal of Heat Transfer*, **101**(4), 718–725 (1979). <https://doi.org/10.1115/1.3451063>
- [2] A. Bejan, and J. Kestin, "Entropy generation through heat and fluid flow," *Journal of Applied Mechanics*, **50**(2), 475 (1983). <https://doi.org/10.1115/1.3167072>
- [3] B.A. Abu-Hijleh, and W.N. Heilen, "Entropy generation due to laminar natural convection over a heated rotating cylinder," *International Journal of Heat and Mass Transfer*, **42**(22), 4225–4233 (1999). [https://doi.org/10.1016/S0017-9310\(99\)00078-2](https://doi.org/10.1016/S0017-9310(99)00078-2)
- [4] S.A. Bayta, "Entropy generation for natural convection in an inclined porous cavity," *International Journal of Heat and Mass Transfer*, **43**(12), 2089–2099 (2000). [https://doi.org/10.1016/S0017-9310\(99\)00291-4](https://doi.org/10.1016/S0017-9310(99)00291-4)
- [5] S. Mahmud, and A.S. Islam, "Laminar free convection and entropy generation inside an inclined wavy enclosure," *International Journal of Thermal Sciences*, **42**(11), 1003–1012 (2003). [https://doi.org/10.1016/S1290-0729\(03\)00076-0](https://doi.org/10.1016/S1290-0729(03)00076-0)
- [6] R.D.C. Oliviski, M.H. Macagnan, and J.B. Copetti, "Entropy generation and natural convection in rectangular cavities," *Applied Thermal Engineering*, **29**(8-9), 1417–1425 (2009). <https://doi.org/10.1016/j.applthermaleng.2008.07.012>
- [7] K. Hooman, and A. Haji-Sheikh, "Analysis of heat transfer and entropy generation for a thermally developing brinkman–brinkman forced convection problem in a rectangular duct with isoflux walls," *International Journal of Heat and Mass Transfer*, **50**(21-22), 4180–4194 (2007). <https://doi.org/10.1016/j.ijheatmasstransfer.2007.02.036>
- [8] T.N. Abdelhameed, "Entropy generation analysis for MHD flow of water past an accelerated plate," *Scientific Reports*, **11**(1), 11964 (2021). <https://doi.org/10.1038/s41598-021-89744-w>
- [9] Z. Khan, O. Makinde, R. Ahmad, and W. Khan, "Numerical study of unsteady MHD flow and entropy generation in a rotating permeable channel with slip and Hall effects," *Communications in Theoretical Physics*, **70**(5), 641 (2018). <https://doi.org/10.1088/0253-6102/70/5/641>
- [10] M. Mansour, S. Siddiqa, R.S.R. Gorla, and A. Rashad, "Effects of heat source and sink on entropy generation and MHD natural convection of  $Al_2O_3$ -Cu/water hybrid nanofluid filled with square porous cavity," *Thermal Science and Engineering Progress*, **6**, 57–71 (2018). <https://doi.org/10.1016/j.tsep.2017.10.014>
- [11] B. Sharma, R. Gandhi, N.K. Mishra, and Q.M. Al-Mdallal, "Entropy generation minimization of higher-order endothermic/exothermic chemical reaction with activation energy on MHD mixed convective flow over a stretching surface," *Scientific Reports*, **12**(1), 17688 (2022). <https://doi.org/10.1038/s41598-022-22521-5>
- [12] S.A. Khan, T. Hayat, M.I. Khan, and A. Alsaeidi, "Salient features of Dufour and Soret effect in radiative MHD flow of viscous fluid by a rotating cone with entropy generation," *International Journal of Hydrogen Energy*, **45**(28), 14552–14564 (2020). <https://doi.org/10.1016/j.ijhydene.2020.03.123>
- [13] G. Shit, R. Haldar, and S. Mandal, "Entropy generation on MHD flow and convective heat transfer in a porous medium of exponentially stretching surface saturated by nanofluids," *Advanced Powder Technology*, **28**(6), 1519–1530 (2017). <https://doi.org/10.1016/j.apt.2017.03.023>

- [14] S. Afsana, M.M. Molla, P. Nag, L.K. Saha, and S. Siddiq, "MHD natural convection and entropy generation of non-Newtonian ferrofluid in a wavy enclosure," *International Journal of Mechanical Sciences*, **198**, 106350 (2021). <https://doi.org/10.1016/j.ijmecsci.2021.106350>
- [15] J. Qing, M.M. Bhatti, M.A. Abbas, M.M. Rashidi, and M.E.-S. Ali, "Entropy generation on MHD Casson nanofluid flow over a porous stretching/shrinking surface," *Entropy*, **18**(4), 123 (2016). <https://doi.org/10.3390/e18040123>
- [16] S. Aiboud, and S. Saouli, "Entropy analysis for viscoelastic magnetohydrodynamic flow over a stretching surface," *International Journal of Non-Linear Mechanics*, **45**(5), 482–489 (2010). <https://doi.org/10.1016/j.ijnonlinmec.2010.01.007>
- [17] S. Hussain, S. Shoeibi, and T. Armaghani, "Impact of magnetic field and entropy generation of Casson fluid on double diffusive natural convection in staggered cavity," *International Communications in Heat and Mass Transfer*, **127**, 105520 (2021). <https://doi.org/10.1016/j.icheatmasstransfer.2021.105520>
- [18] M.H. Yazdi, S. Abdullah, I. Hashim, and K. Sopian, "Entropy generation analysis of open parallel microchannels embedded within a permeable continuous moving surface: application to magnetohydrodynamics (MHD)," *Entropy*, **14**(1), 1–23 (2011). <https://doi.org/10.3390/e14010001>
- [19] M.H. Yazdi, S. Abdullah, I. Hashim, and K. Sopian, "Reducing entropy generation in MHD fluid flow over open parallel microchannels embedded in a micropatterned permeable surface," *Entropy*, **15**(11), 4822–4843 (2013). <https://doi.org/10.3390/e15114822v>
- [20] M. Rashidi, N. Kavyani, and S. Abelman, "Investigation of entropy generation in MHD and slip flow over a rotating porous disk with variable properties," *International Journal of Heat and Mass Transfer*, **70**, 892–917 (2014). <https://doi.org/10.1016/j.ijheatmasstransfer.2013.11.058>

**ЧИСЛОВИЙ АНАЛІЗ ГЕНЕРАЦІЇ ЕНТРОПІЇ МГД ПОТОКОМ РІДИНИ КАССОНА  
ЧЕРЕЗ ПОХИЛУ ПЛАСТИНУ З ЕФЕКТОМ СОРЕ**

**Хірен Дека, Парісміта Пхукан, Пуджа Халой**

*Факультет математики, Університет Коттон, Ассам, Індія*

У цьому дослідженні досліджується генерація ентропії для нестационарного МГД потоку рідини Кассона через коливальну похилу пластину. Тут, поряд з реакцією хімічним і тепловим випромінюванням, також аналізується включення ефекту Сорє. Розв'язок рівняння, яке керує проблемою потоку, отримано методом кінцевих різниць (FDM). Характеристики швидкості потоку, концентрації та температури аналізуються шляхом побудови графіків, а їх фізична поведінка детально розглядається для вивчення впливу різних параметрів на проблему рідини. Тертя шкіри, швидкість тепло- та масообміну рідини також мають значний вплив під впливом параметрів. Результати показують, що ефект Сорє та інші параметри мають значний вплив на нестационарну МГД кассонову рідину та на загальну ентропію через теплообмін і тертя потоку.

**Ключові слова:** ентропія; Кассон; МГД; ефект Сорє; теплове випромінювання